Broadband Analysis of Microwave Structures by Enhanced Finite-Element Methods

Milan MOTL [*], *Zbyněk RAIDA*

Dept. of Radio Electronics, Brno University of Technology, Purkyňova 118, 612 00 Brno, Czech Republic

milan.motl@cz.flextronics.com, raida@feec.vutbr.cz

Abstract. *The paper deals with the broadband modeling of microwave structures by finite-element methods. The attention is turned to original enhancements of accuracy, efficiency and stability of finite-element codes.*

The partial improvements are based on novel approximations both in the spatial domain and in the time one, in the adoption of complex frequency hopping, fast frequency sweep and envelope finite-element techniques. In the paper, a possible hybridization of approaches is discussed.

Proposed finite-element schemes are applied to the analysis of canonical longitudinally homogeneous transmission lines in order to demonstrate their advantages.

Keywords

Finite-element method, broadband modeling, time-domain modeling, complex frequency hopping, envelope finite elements, fast frequency sweep.

1. Introduction

Numerical analysis of microwave structures can be performed in the frequency domain or in the time domain.

In the frequency domain, the problem formulation is based on Maxwell's equations assuming the harmonic nature of all the quantities [1]–[3]. Consequently, the formulation does not contain time derivatives, which are represented by the complex frequency multiplication. The frequency-domain analysis is therefore relatively simple and CPU-time modest.

The time-domain analysis assumes a general time behavior of both the excitations and the responses [4]–[6]. The time-domain formulation increases the dimension of the problem and complicates the solution (time derivatives of the computed quantities appear). The time domain ana-lysis is therefore more complex and time demanding. On the other hand, if the microwave structure is going to be analyzed in a relative wide band of frequencies, the result can be obtained within a single run of the time domain analysis (if the structure is excited by a narrow pulse containing those frequencies); this is more efficient compared to several runs of independent frequency-domain analyses.

In the paper, we concentrate on differential methods.

At the present, finite difference time domain method (FDTD) is dominant in the area of differential time domain methods [7], [8]. FDTD is based on the approximation of partial derivatives in Maxwell's equations (both in the time and in the space) by central finite differences. Thanks to the ingenious discretization cell proposed by Yee [9], obtained solutions naturally meet the third Maxwell's equation and the fourth one, and the computational algorithm is extremely efficient. On the contrary, FDTD computes electromagnetic field in nodes of the discretization mesh only. Modeling of curved surfaces is rather problematic, and building inhomogeneous discretization meshes brings difficulties [4].

As shown in [5], all the described problems of FDTD are removed by time domain finite elements (TDFE). Moreover, we can create a TDFE scheme, which is absolutely stable for an arbitrary length of the spatial step and the temporal one [5].

The paper concentrates on TDFE, which is based on solving the wave equation in the time domain. For the electric field intensity inside the analyzed volume, the wave equation is of the form [10]

$$-\mu_0 \frac{\partial \mathbf{J}_i(\mathbf{r},t)}{\partial t} = \nabla \times \left[\frac{1}{\mu_r} \nabla \times \mathbf{E}(\mathbf{r},t) \right] +$$

$$+ \mu_0\, \varepsilon_0\, \varepsilon_r \frac{\partial^2 \mathbf{E}(\mathbf{r},t)}{\partial t^2} + \mu_0 \sigma \frac{\partial \mathbf{E}(\mathbf{r},t)}{\partial t} , \qquad (1)$$

where $\mathbf{E}$ is the electric field intensity vector, $\mu = \mu_0\, \mu_r$ de-

notes permeability, $\varepsilon = \varepsilon_0\,\varepsilon_r$ is permittivity, and σ is conductivity inside the analyzed volume. The vector $\mathbf{J}_i$ represents the excitation current density, $\mathbf{r}$ is the position vector and t denotes time.

In order to obtain a unique solution, the wave equation (1) has to be completed by boundary conditions on the surface Γ around the analyzed volume Ω. Generally, boundary conditions can be expressed in the form [10]

$$\mathbf{U}(\mathbf{r},t) = Y \frac{\partial}{\partial t}\big[\mathbf{n}\times\mathbf{n}\times\mathbf{E}(\mathbf{r},t)\big] + \\ + \mathbf{n}\times\left[\frac{1}{\mu}\nabla\times\mathbf{E}(\mathbf{r},t)\right], \quad (2)$$

where $\mathbf{n}$ is the unitary vector, which is perpendicular to the surface Γ surrounding the analyzed volume Ω, Y represents the surface admittance of the surface Γ, and $\mathbf{U}$ is a known value representing sources on Γ.

When applying the general TDFE scheme [4], [5] to the solution of (1) with respect to (2), the volume Ω is subdivided to tetrahedrons (finite elements) and the computed quantity is formally approximated over tetrahedrons: known basis functions[1] $\mathbf{N}_i(\mathbf{r})$ are multiplied by unknown approximation coefficients[2] $e_i(t)$. Since the approximation does not meet the wave equation (1) perfectly, a residual term has to be added to the left-hand side of (1). Since the minimum residual error corresponds to the most accurate solution of (1), the residual is consequently minimized.

The residual error can be minimized by the method of weighted residua [13], [14]: the error is multiplied by weighting functions $\mathbf{W}_j(\mathbf{r})$, the product is integrated over the analyzed volume Ω, and the result is set to zero. If the error is weighted as many times as many unknown approximation coefficients we have (N), Maxwell's equations are converted to the set of N algebraic equations in the general form [10]

$$\mathbf{T}\cdot\frac{\partial^2\mathbf{E}(t)}{\partial t^2} + \mathbf{B}\cdot\frac{\partial\mathbf{E}(t)}{\partial t} + \mathbf{S}\cdot\mathbf{E}(t) + \mathbf{f}(t) = 0 , \quad (3)$$

where $\mathbf{E}(t)$ is column vector of temporal responses of the approximation coefficients of the finite-element method,

i.e. $\mathbf{E}(t) = [e_1(t), e_2(t), ..., e_N(t)]^{\mathrm{T}}$. Elements of the vector $\mathbf{f}$ representing sources is given by [10]

$$f_i(t) = \mu_0\int_\Omega \mathbf{W}_i(\mathbf{r})\cdot\frac{\partial\mathbf{J}(\mathbf{r},t)}{\partial t}\,d\Omega , \quad (4a)$$

and elements of matrices $\mathbf{T}$, $\mathbf{S}$, and $\mathbf{B}$ can be evaluated following [10]

$$T_{ij} = \frac{1}{c^2}\int_\Omega \varepsilon_r\,\mathbf{W}_i(\mathbf{r})\cdot\mathbf{N}_j(\mathbf{r})d\Omega , \quad (4b)$$

$$S_{ij} = \int_\Omega \big[\nabla\times\mathbf{W}_i(\mathbf{r})\big]\cdot\frac{1}{\mu_r}\big[\nabla\times\mathbf{N}_j(\mathbf{r})\big]d\Omega , \quad (4c)$$

$$B_{ij} = R_{ij} + Q_{ij} ,$$

where

$$R_{ij} = \frac{1}{c}\int_\Gamma \sqrt{\frac{\varepsilon_r}{\mu_r}}\big[\mathbf{W}_i(\mathbf{r})\times\mathbf{n}\big]\cdot\big[\mathbf{N}_j(\mathbf{r})\times\mathbf{n}\big]d\Omega , \quad (4d)$$

$$Q_{ij} = \mu_0\int_\Omega \sigma\,\mathbf{W}_i(\mathbf{r})\cdot\mathbf{N}_j(\mathbf{r})d\Omega . \quad (4e)$$

In (4), $\mathbf{W}_i(\mathbf{r})$ are vectorial weighting functions, and $\mathbf{N}_j(\mathbf{r})$ are vectorial basis ones, Ω represents the volume of the analysis, and Γ is the surface surrounding the volume Ω, $\mathbf{J}(\mathbf{r}, t)$ denotes the vector of the source current density, $\mu = \mu_0\,\mu_r$ denotes permeability, $\varepsilon = \varepsilon_0\,\varepsilon_r$ is permittivity, and σ is conductivity inside the analyzed volume, $\mathbf{n}$ is a normal to the surface Γ, and c is the velocity of light.

Solving the algebraic problem (3), the column vector of unknown approximation coefficients $\mathbf{E}(t)$ is obtained.

Accuracy of the analysis is significantly influenced by used basis functions and weighting ones [3]. In order to reduce the error of the analysis, we propose special quasi-cubic basis functions and weighting ones (a more accurate spatial field distribution), and we introduce a high-order approximation in time (a more accurate temporal field distribution). Details are given in Section 2 of the paper.

In order to enhance the efficiency of the finite element code, we combine the finite element analysis and the concept of complex frequency hoping [15], [16]. Details are given in Section 3 of the paper.

Time domain analyses produce time responses of computed field quantities. Since the conventional parameters of microwave structures (scattering parameters, impedances, directivity patterns, gains, etc.) are formulated in the frequency domain, time responses are usually processed by fast Fourier transform (FFT), which increase computational demands and decrease the accuracy of the analysis by an additional error. In order to overcome this difficulty, we propose a direct time domain computation of parameters as explained in Section 4.

Section 5 is devoted to proposing an original hybrid method, which combines fast frequency sweep and enve-

---

[1]   In the general formulation, the basis functions are of the vectorial *edge* nature [11], [12]. Edge basis functions consist of unitary vectors, which are oriented to the directions of edges of finite elements. This construction ensures continuity of field components on the interface of dielectric layers.

[2]   Basis functions do not depend on time because the analyzed structure is time-invariant. When performing time-domain analysis, the computed field is not in the steady state, and hence the approximation *coefficients* are functions of time.

lope finite elements [17]–[19]. Properties of the novel hybrid method are compared with conventional approaches.

Section 6 concludes the paper.

2. Enhancing Accuracy of TDFE

Numerical analysis in the time domain is accurate when providing an accurate spatial distribution of computed field quantities (e.g., field intensity inside the volume Ω of an analyzed cavity resonator), and also accurate time responses of those quantities (e.g., time response of field intensity inside a cavity resonator excited by a Gaussian pulse). Spatial accuracy can be enhanced by using special basis functions and weighting ones, temporal accuracy can be improved using high-order approximations of time behavior.

2.1 Quasi-Cubic Basis and Weighting Functions

Novel basis and weighting functions are going to be explained in modal analysis[3] of a longitudinally homogeneous waveguide consisting of perfectly electrically conductive (PEC) walls in the vacuum. Since there are no interfaces of dielectric layers in the analyzed structure, edge basis and weighting functions can be replaced by nodal ones [3]. Due to the longitudinal homogeneity, the cross-section of the waveguide is satisfactory to be discretized by two-dimensional triangular finite elements.

Then, the general finite-element solution (3) of the wave equation (1) can be rewritten to the form [20]

$$\mathbf{SE} + \left(k_0^2 - \beta^2\right)\mathbf{TE} = 0 \tag{5}$$

where $\mathbf{E}$ is the column vector of nodal values of electric field intensity, k_0 denotes free space wave number, and β is phase propagation constant. Matrices of coefficients $\mathbf{S}$ and $\mathbf{T}$ (see the general form 4b, c) can be now expressed as

$$\mathbf{T}^{(e)} = A^{(e)} \begin{bmatrix} t_1 & t_2 & t_2 \\ t_2 & t_1 & t_2 \\ t_2 & t_2 & t_1 \end{bmatrix} \tag{6a}$$

$$\mathbf{S}^{(e)} = \sum_{n=1}^{3} \mathbf{Q}_n \cotg\left[\vartheta_n^{(e)}\right] \tag{6b}$$

where $A^{(e)}$ denotes the area of the e-th finite element, $\vartheta_n^{(e)}$ is the n-th angle of the e-th finite element, the matrix $\mathbf{Q}_1$ is given as

---

3 Modal analysis can be used for evaluating critical (eigen)frequencies and field distributions of corresponding (eigen)modes. In case of a longitudinally homogeneous transmission line, transversal resonances are investigated in a fact [20].

$$\mathbf{Q}_1 = \begin{bmatrix} 0 & 0 & 0 \\ 0 & q_1 & q_2 \\ 0 & q_2 & q_1 \end{bmatrix} \tag{6c}$$

and $\mathbf{Q}_2$, $\mathbf{Q}_3$ can be obtained by permuting $\mathbf{Q}_1$. Coefficients t_1, t_2, q_1 and q_2 in (6) depend on the type of basis and weighting functions used. For low-order splines (linear, quadratic and cubic ones), the coefficients are simple rational constants.

Comparing the purely quadratic spline and the purely cubic one, both of them contain a negative quadratic term, and both of them equal 1 for $x = 0$. Considering this fact, we can create a more general quasi-cubic spline

$$\begin{aligned} y &= -ax^3 - bx^2 + 1 & x \in \langle -1;0 \rangle \\ y &= ax^3 - bx^2 + 1 & x \in \langle 0;1 \rangle \end{aligned} \tag{7}$$

that is continuous and smooth over the finite element.

Following the finite-element procedure, quasi-cubic splines (7) are integrated, and coefficients t_1, t_2, q_1, q_2 from (6) are expressed in the form of functions depending on parameters b_1 and b_2. Next, we consider the basis functions are zero for $x = \pm 1$, splines behave anti-symmetrically, and the basis functions differ from weighting ones.

Enforcing the analysis to converge to the exact solution of (1) for infinitely small finite elements, the following values of the coefficients t_1, t_2, q_1, q_2 are obtained:

$$q_1 = +0.658\,637\,54 , \tag{8a}$$

$$q_2 = -0.658\,637\,54 , \tag{8b}$$

$$t_1 = +0.226\,526\,51 , \tag{8c}$$

$$t_2 = +0.106\,288\,41 . \tag{8d}$$

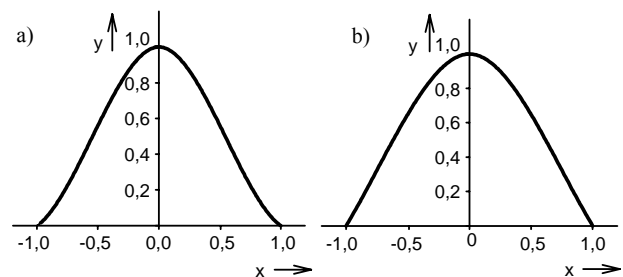The derived quasi-cubic basic function and the weighting one are depicted in Fig. 1.

Fig. 1.   The proposed quasi-cubic basis function (a) and the quasi-cubic weighting function (b).

Properties of the developed quasi-cubic functions were tested on the analysis of the rectangular, longitudinally homogeneous waveguide R100. Results are depicted in Fig. 2 and compared with linear basis and weighting functions (Galerkin's approach).

Fig. 2 proves a better accuracy of quasi-cubic splines for the discretization mesh consisting of 22×10 rectangu-

lar cells, which are composed from two triangular finite elements.

Similar results are obtained when using quasi-cubic splines for approximating the spatial distribution of the electromagnetic field in the TDFE method [21], [22]. Hence, the novel quasi-cubic functions can be concluded to be advantageous both in the modal analysis and in the time-domain one.
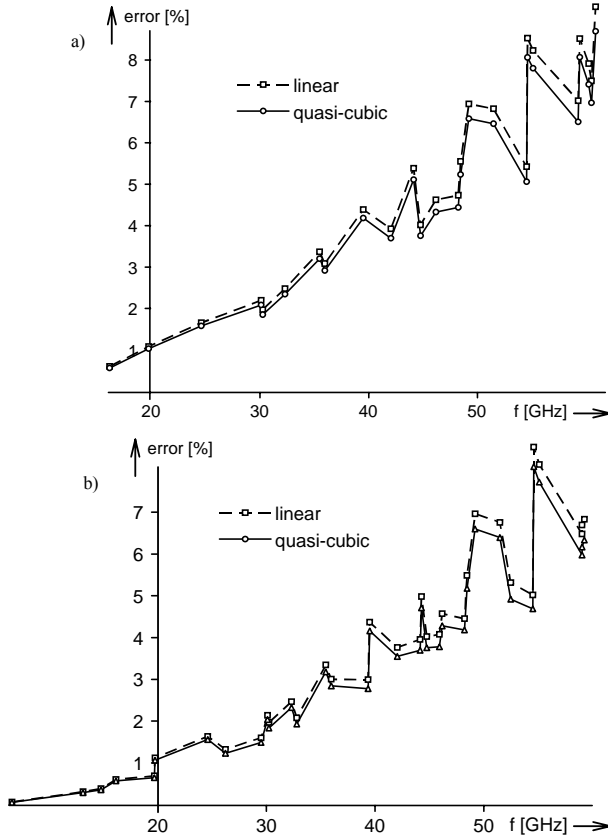
Fig. 2. Percentage error in the resonant frequency of the rectangular waveguide R100 for the transversally magnetic modes (a) and the transversally electric modes (b). The cross section of the waveguide was divided to 22 × 10 rectangular cells, which consist of two triangular finite elements.

In the next paragraph, we turn our attention to the approximation of time responses in the TDFE analysis.

2.2 High-Order Temporal Approximations

When time responses of field quantities are going to be evaluated, highly accurate approximation of their spatial distribution has to be accompanied by highly accurate approximation of temporal responses also.

The most common TDFE versions [5] approximate the computed time response by a second-order polynomial resulting in a two-step algorithm. If a more general algorithm is going to be developed, higher-order polynomials have to be applied. In the paper, we concentrate on the three-step approach.

A novel three-step algorithm will be explained in the analysis of a three-dimensional cavity resonator consisting of PEC walls in the vacuum. For modeling purposes, tetrahedral nodal elements will be used [3].

The formulation of the third-order approximation is based on Lagrange polynomials [3]. Due to symmetry, nodal values of the computed quantity e, which correspond to equidistant time instants $-3\delta t/2$, $-\delta t/2$, $\delta t/2$, $3\delta t/2$, are denoted as e^{-2}, e^{-1}, e^1 a e^2, and the polynomial is of the form [21]

$$
\begin{aligned}
\left[48 \left(\delta t\right)^3 \right] e(t) = \\
= \big[a\, e^{-2} \left(2t+\delta t\right)\left(2t-\delta t\right)\left(2t-3\delta t\right) + \\
+\ b\, e^{-1} \left(2t+3\delta t\right)\left(2t-\delta t\right)\left(2t-3\delta t\right) + \\
+\ c\, e^{+1} \left(2t+3\delta t\right)\left(2t+\delta t\right)\left(2t-3\delta t\right) + \\
+\ d\, e^{+2} \left(2t+3\delta t\right)\left(2t+\delta t\right)\left(2t-\delta t\right)\big]
\end{aligned}
\tag{9}
$$

Here $e(t)$ is the continuous temporal approximation of the quantity e, superscripts denote the indexes of time samples of e, δt is the sampling step, and t is time. Comparing functional values of derivatives of $e(t)$ in nodes and values of corresponding finite differences, we obtain $a = -1$, $b = 3$, $c = -3$, and $d = 1$.

We evaluate the first and the second derivative of (9), substitute them to the semi-discrete equation (3), and perform the time weighting of the residual. Enforcing the stability conditions, we can formulate:

- Symmetric implicit algorithm

$$
\begin{aligned}
&\left[\frac{1}{2}\mathbf{T} - \frac{1}{3}\left(\delta t\right)\mathbf{B} + \frac{1}{8}\left(\delta t\right)^2\mathbf{S}\right] \mathbf{E}^{n-2} + \\
&+ \left[-\frac{1}{2}\mathbf{T} + \frac{3}{8}\left(\delta t\right)^2\mathbf{S}\right] \mathbf{E}^{n-1} + \\
&+ \left[-\frac{1}{2}\mathbf{T} + \frac{3}{8}\left(\delta t\right)^2\mathbf{S}\right] \mathbf{E}^{n} + \\
&+ \left[\frac{1}{2}\mathbf{T} + \frac{1}{3}\left(\delta t\right)\mathbf{B} + \frac{1}{8}\left(\delta t\right)^2\mathbf{S}\right] \mathbf{E}^{n+1} = \left(\delta t\right)^2 \mathbf{f}
\end{aligned}
\tag{10a}
$$

- Symmetric explicit algorithm

$$
\begin{aligned}
&\left[\frac{1}{2}\mathbf{T} - \frac{1}{12}\left(\delta t\right)\mathbf{B}\right] \mathbf{E}^{n-2} + \\
&+ \left[-\frac{1}{2}\mathbf{T} - \frac{3}{4}\left(\delta t\right)\mathbf{B} + \frac{1}{2}\left(\delta t\right)^2\mathbf{S}\right] \mathbf{E}^{n-1} + \\
&+ \left[-\frac{1}{2}\mathbf{T} + \frac{3}{4}\left(\delta t\right)\mathbf{B} + \frac{1}{2}\left(\delta t\right)^2\mathbf{S}\right] \mathbf{E}^{n} + \\
&+ \left[\frac{1}{2}\mathbf{T} + \frac{1}{12}\left(\delta t\right)\mathbf{B}\right] \mathbf{E}^{n+1} = \left(\delta t\right)^2 \mathbf{f}
\end{aligned}
\tag{10b}
$$

- Non-symmetric implicit algorithm

$$\left[-\frac{1}{12}(\delta t)\, \mathbf{B} \right] \mathbf{E}^{n-2} +$$

$$+ \left[\mathbf{T} - \frac{1}{4}(\delta t)\, \mathbf{B} + \frac{1}{4}(\delta t)^2 \mathbf{S} \right] \mathbf{E}^{n-1} +$$

$$+ \left[-2\mathbf{T} - \frac{1}{4}(\delta t)\, \mathbf{B} + \frac{1}{2}(\delta t)^2 \mathbf{S} \right] \mathbf{E}^{n} + \tag{10c}$$

$$+ \left[\mathbf{T} + \frac{7}{12}(\delta t)\, \mathbf{B} + \frac{1}{4}(\delta t)^2 \mathbf{S} \right] \mathbf{E}^{n+1} = (\delta t)^2 \mathbf{f}$$

- Non-symmetric explicit algorithm

$$\left[\frac{1}{6}(\delta t)\, \mathbf{B} \right] \mathbf{E}^{n-2} +$$

$$+ \left[\mathbf{T} - (\delta t)\, \mathbf{B} \right] \mathbf{E}^{n-1} +$$

$$+ \left[-2\mathbf{T} + \frac{1}{2}(\delta t)\, \mathbf{B} + (\delta t)^2 \mathbf{S} \right] \mathbf{E}^{n} + \tag{10d}$$

$$+ \left[\mathbf{T} + \frac{1}{3}(\delta t)\, \mathbf{B} \right] \mathbf{E}^{n+1} = (\delta t)^2 \mathbf{f}$$

- Fully explicit algorithm

$$\left[\frac{1}{2}\mathbf{T} - \frac{1}{12}(\delta t)^2 \mathbf{S} \right] \mathbf{E}^{n-2} +$$

$$+ \left[-\frac{1}{2}\mathbf{T} - (\delta t)\, \mathbf{B} + \frac{2}{3}(\delta t)^2 \mathbf{S} \right] \mathbf{E}^{n-1} +$$

$$+ \left[-\frac{1}{2}\mathbf{T} + (\delta t)\, \mathbf{B} + \frac{5}{12}(\delta t)^2 \mathbf{S} \right] \mathbf{E}^{n} + \tag{10e}$$

$$+ \left[\frac{1}{2}\mathbf{T} \right] \mathbf{E}^{n+1} = (\delta t)^2 \mathbf{f}$$

In (10), matrices $\mathbf{T}$, $\mathbf{B}$, $\mathbf{S}$ and $\mathbf{f}$ are given by relations (4) with vectorial edge basis functions $\mathbf{N}(\mathbf{r})$ and weighting ones $\mathbf{W}(\mathbf{r})$ replaced by scalar nodal basis functions $N(\mathbf{r})$ and weighting ones $W(\mathbf{r})$. Next, $\mathbf{E}^n$ is column vector of the n-th time sample of the finite-element approximation coefficients, i.e. $\mathbf{E}^n = [e_1^n, e_2^n, ..., e_N^n]^{\mathrm{T}}$. Finally, δt denotes the temporal sampling period.

Symmetrical algorithms (10a), (10b) were derived to reduce the dispersion error of the analysis; those expectations were not fulfilled. On the other hand, the explicit algorithm (10b) exhibits better stability compared to the conventional two-step algorithm.

Algorithms (10) were tested analyzing a rectangular resonator of dimensions 150 mm × 180 mm × 130 mm. The resonator volume was divided into 20 × 20 × 20 finite elements. The resonator was analyzed within the frequency range from 0 to 4 GHz with the frequency step 0.5 MHz. Analysis was performed using the conventional two-step

algorithms and the proposed three-step ones. For comparison purposes, results of the analyses were transformed to the frequency domain, and computed spectra were compared (see Fig. 3). Obviously, they produce identical results.
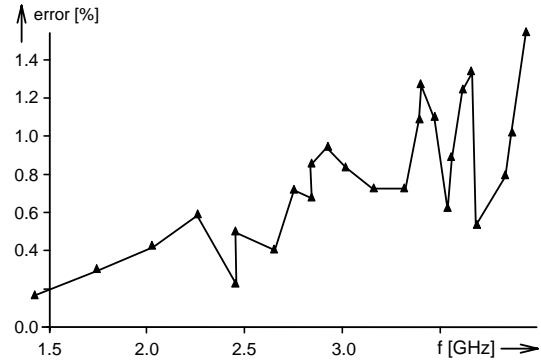

Fig. 3. Dispersion error of resonant frequencies of the rectangular cavity resonator using a two-step algorithm and three-step algorithms (10). Results are identical.

Non-symmetrical algorithms (10c) and (10d) were derived for the analysis of lossy structures, structures containing perfectly matched layers, or structures terminated by absorbing boundary conditions. For closed lossless structures, (10c) and (10d) are identical with the conventional two-step algorithms in the explicit form or the implicit one. The fully explicit algorithm (10e) was derived for the potential time-domain hybridization of finite elements and boundary integrals [21], [24].

3. Enhancing Efficiency of TDFE

In the previous section, we discussed ways of enhancing accuracy of the finite-element analysis by improving spatial and temporal approximations of electromagnetic fields. In this section, we concentrate on improving efficiency of the analysis. For that purpose, we originally adopt the technique known as the Complex Frequency Hopping (CFH) [15].

The CFH method understands the analyzed structure as a transmission system, which transfer function is approximated in Laplace domain. Accuracy of the approximation is consequently increased using Padé approximation and hops of complex frequency [15].

Adoption of CFH for finite-element analysis will be explained on modeling longitudinally homogeneous transmission lines. Hence, two-dimensional triangular elements are used for discretizing cross-section of the analyzed waveguide.

For the described situation, we solve again the wave equation (1), which is converted by the finite element approach to the matrix form (3). In the next step, (3) is transformed to Laplace domain [25]

$$\left[\mathbf{T}s^2 + \mathbf{B}s + \mathbf{S} \right] \cdot \mathbf{X}(s) = \mathbf{R}(s) , \tag{11}$$

where s denotes complex frequency, matrices $\mathbf{T}$, $\mathbf{B}$, and $\mathbf{S}$ are given by (4), $\mathbf{X}(s) = L\{\mathbf{E}(t)\}$ is Laplace image of the column vector of unknown field temporal responses, and $\mathbf{R}(s)$ is Laplace image of excitation vector

$$\mathbf{R}(s) = s\mathbf{T} \cdot [\mathbf{E}_0 + \mathbf{E}'_0] + \mathbf{B} \cdot \mathbf{E}_0 + \mathbf{F}(s) \tag{12}$$

with $\mathbf{F}(s) = L\{\mathbf{f}(t)\}$, $\mathbf{E}_0$ is the initial value of the vector $\mathbf{E}$, and $\mathbf{E}'_0$ is the value of the first derivative in instant $t = 0$.

Equation (11) is formally identical with the description of a linear system. The excitation vector $\mathbf{R}(s)$ corresponds to the input signals, the vector of unknown temporal responses $\mathbf{X}(s)$ corresponds to the output signals, and the transfer function is given by $\mathbf{H}^{-1}(s) = \mathbf{T}s^2 + \mathbf{B}s + \mathbf{S}$.

Padé approximation is based on the expansion of the transfer function $\mathbf{H}(s)$ in the investigated frequency band to Taylor series [3.1]. The investigated frequency band is sequentially divided to subintervals, transfer function is approximated on subintervals, and its functional values are compared on the borders of those subintervals. The sequential dividing continues as long as the differences of the approximation on the borders of subintervals do not meet the prescribed value.
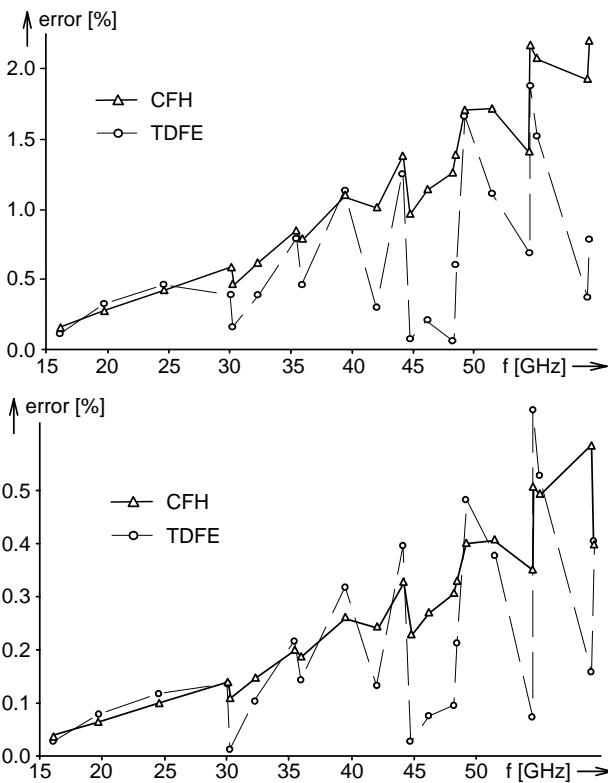
Fig. 4. Percentage error in the resonant frequency of the rectangular waveguide R100 for the transversally magnetic modes (top) and the transversally electric modes (bottom). The cross section of the waveguide was divided to 44×20 rectangular cells (top) and 88×40 cells (bottom). Rectangular cells consist of two triangular finite elements.

CFH performance was tested in the modal analysis of the waveguide R100. In Fig. 4, percentage error of critical frequencies of transversally magnetic (top) and transversally electric (bottom) modes is depicted. CFH values are related to the results of the TDFE analysis performed on the twice-sparser finite-element mesh.

	44×20 vs. 22×10	88×40 vs. 44×20
CFH	30.7	211.5
TDFE	90.2	720.5

Tab. 1. CPU-time demands of CFH versus TDFE in the modal analysis of the waveguide R100. In case of TDFE, the twice-sparser finite-element mesh was used.

Results show TDFE more accurate compared to CFH: for the twice-denser finite-element mesh, CFH produced comparable percentage error than TDFE. On the other hand, CPU-time demands of TDFE are much higher even if a twice-sparser mesh compared to CFH is used [26], [27].

4. Time Domain Evaluation of Parameters

Most parameters, which are used for the description of microwave systems, are evaluated and formulated in the frequency domain (impedance, directivity patterns, scattering parameters, etc.). If the numerical analysis is performed in time domain, time responses of computed quantities contain discrete frequency components from the whole frequency band excited by the excitation pulse. In order to evaluate conventional parameters, time responses have to be transformed in the Fourier sense, and isolated harmonics have to be used for evaluating frequency-domain parameters. Such an approach decreases efficiency and accuracy of the time-domain approach. In order to solve the described problem, Envelope Finite Elements (EVFE) [17]–[19] are originally adopted in this paper.

Adoption of EVFE for time-domain analysis and consequent time-domain parameter evaluation will be demonstrated on computing wave impedance of a longitudinally homogeneous transmission line. Hence, a two-dimensional problem is again solved.

In the original formulation of the EVFE, field components and sources are expressed in the form [17]–[19]

$$U(t) = V(t)\exp[j\omega_c t], \tag{13}$$

where $U(t)$ is a field/source component, $V(t)$ denotes time-dependent complex envelope of that quantity, and ω_c is carrier frequency.

In the presented approach, field/source components are assumed in the form of the product of two functions. The first function v depends on transversal spatial components x, y and time t, the second component Φ depends on the longitudinal spatial component z and time t. The temporal dimension enables the formulation of transient phenomena, spatial dimensions are separated in order to model well the wave propagation in longitudinally homogeneous transmission lines [21].

For the magnetic field intensity vector, we get

$$H(x,y,z,t) = h(x,y,t)\,\Phi(z,t)\ . \tag{14}$$

Similarly, electric field intensity vector $\mathbf{E} = [e_x, e_y, e_z]^T$ and sources $\mathbf{J} = [j_x, j_y, j_z]^T$ can be described; the term $\Phi(z, t)$ is shared by all the quantities.

Terms $\mathbf{H}$ in the formulation (14) and sources $\mathbf{J}$ are substituted to the wave equation (1), which is formulated for magnetic field intensity vector. Then, the equation is solved.

In order to make the equation solvable, time independence of terms containing Φ has to be assumed. This yields the condition [21]

$$\Phi(z,t) = \exp(-\gamma_c\,z)\,\exp(j\,\omega_c\,t) \tag{15}$$

with the complex propagation constant γ_c (longitudinal direction, carrier ω_c). Several mathematical rearrangements and simplifications yield [21]

$$
-\left(\frac{\partial j_x}{\partial y} - \frac{\partial j_y}{\partial x}\right) =
$$
$$
= \left[\frac{\partial^2 h_z}{\partial x^2} + \frac{\partial^2 h_z}{\partial y^2}\right] + \left(\gamma_c^2 + k_c^2\right) h_z -
$$
$$
- \mu\left[2j\varepsilon\omega_c + \sigma\right]\frac{\partial h_z}{\partial t} - \mu\varepsilon\,\frac{\partial^2 h_z}{\partial t^2}\ , \tag{16}
$$

where $\mathbf{J}_t = [j_x, j_y]^T$ are transversal component of the current source, h_z is the longitudinal component of the magnetic field intensity, γ_c is the complex propagation constant in the longitudinal direction, k_c denotes free-space wave number for carrier frequency ω_c. Finally, μ, ε, and σ denote permeability, permittivity and conductivity of media inside the analyzed structure.

Applying finite-element procedure to (16), we obtain the EVFE magnetic field alternative of (3) [21]

$$
0 = \tilde{\mathbf{f}} +
$$
$$
+ \left[\frac{1}{\mu_0\,\varepsilon_0}\,\mathbf{T}\right] \cdot \frac{\partial^2 \mathbf{H}}{\partial t^2} +
$$
$$
+ \left[\left(2j\omega_c + \frac{\sigma}{\varepsilon}\right)\frac{1}{\mu_0\,\varepsilon_0}\,\mathbf{T}\right] \cdot \frac{\partial \mathbf{H}}{\partial t} +
$$
$$
+ \left[\mathbf{S} - \left(\gamma_c^2 + k_c^2\right)\frac{c^2}{\mu_r\,\varepsilon_r}\,\mathbf{T}\right] \cdot \mathbf{H} \tag{17}
$$

with

$$\tilde{f}_i = \int_\Omega W_i\,(\nabla \times \mathbf{J})_z\ d\Omega\ . \tag{18}$$

Matrices $\mathbf{S}$ and $\mathbf{T}$ are given by (4), and the column vector of finite-element coefficients is $\mathbf{H} = [h_1, h_2, ..., h_N]^T$.

Time derivatives in (17) are handled by two-step implicit algorithm [21].

When time responses of the longitudinal component of the magnetic field intensity h_z are known, wave impedance of the analyzed transmission line can be evaluated [28]. First, auxiliary integrals are numerically handled [21]

$$
I_{1,i} = \exp\left[-(s + \gamma_c\,c)t_c\right] \cdot
$$
$$
\cdot \int_0^{t_c} \frac{\partial h_{z,i}(t)}{\partial x}\,\exp\left[(s + \gamma_c\,c)\,t\right]\,dt\ , \tag{19a}
$$

$$
I_{2,i} = \exp\left[-(s - \gamma_c\,c)t_c\right] \cdot
$$
$$
\cdot \int_0^{t_c} \frac{\partial h_{z,i}(t)}{\partial x}\,\exp\left[(s - \gamma_c\,c)\,t\right]\,dt\ . \tag{19b}
$$

Second, transversal field components are computed [21]

$$\mathbf{e}_y(n) = \frac{1}{2\,\varepsilon}\,\left[\mathbf{I}_1 + \mathbf{I}_2\right]\ , \tag{20a}$$

$$\mathbf{h}_x(n) = \frac{c}{2}\,\left[\mathbf{I}_1 - \mathbf{I}_2\right]\ . \tag{20b}$$

Third, wave impedance can be evaluated [21]

$$\mathbf{Z}_0 = \frac{\text{FFT}(\mathbf{e}_y)}{\text{FFT}(\mathbf{h}_x)}\ . \tag{21}$$

Here, FFT denotes fast Fourier transform.

Functionality of the method was tested on the analysis of the longitudinally homogeneous rectangular waveguide R100. For the analysis, the finite-element mesh consisting of 22×10 rectangular cells was used. Wave impedance of the dominant mode TE10 was evaluated from the critical frequency to 13 GHz, and was compared to the analytically computed values.

The obtained results demonstrate that EVFE can be applied to the analysis of longitudinally homogeneous transmission lines and the evaluation of wave impedance. The percentage error is minimal at the central frequency, and rises with the increasing distance from it [21], [29].
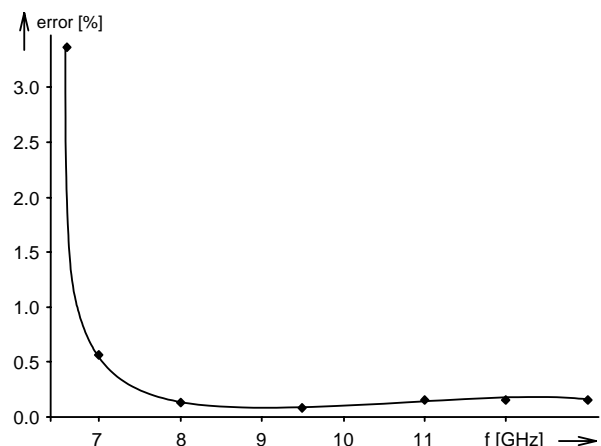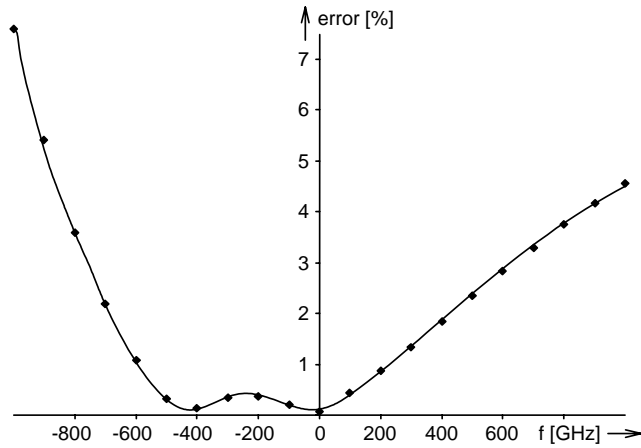

Fig. 5. Percentage error of the numerically evaluated wave impedance of the waveguide R100 on discrete frequencies (related to analytic results).

Fig. 6. Percentage error of the numerically evaluated wave impedance of the waveguide R100 during the broadband analysis on the central frequency 9.5 GHz (corresponds to zero frequency in the chart).

5. Hybrid Methods

Hybrid methods are very popular in today's computational electromagnetics: mutual combination of different approaches can yield a combination of their advantageous features and elimination of their drawbacks.

In section 4, we demonstrated the ability of Envelope Finite Elements (EVFE) to perform an accurate analysis within a relatively broad band of frequencies. In section 3, we applied the concept of Complex Frequency Hopping (CFH) to enhancing efficiency of the finite-element code. Hybridizing EVFE and CFH, a broadband accurate and efficient finite-element modeling tool can be obtained. The novel method is called here Fast Frequency Sweep – Envelope Finite Elements (FFS-EVFE).

Adoption of FFS-EVFE for finite-element analysis will be explained on modeling longitudinally homogeneous transmission lines. Hence, two-dimensional triangular elements are used for discretizing cross-section of the analyzed waveguide.

Solving the wave equation (1), we substitute the electric field intensity vector and the source current in the envelope form (13) there. Applying finite-element procedure, we obtain the FFS-EVFE alternative of (3) [21]

$$0 = \hat{\mathbf{f}} + \mathbf{T} \cdot \frac{\partial^2 \hat{\mathbf{E}}}{\partial t^2} +$$
$$+ \left[\mathbf{R} + 2j\omega_c \mathbf{T}\right] \cdot \frac{\partial \hat{\mathbf{E}}}{\partial t} + \qquad (22)$$
$$+ \left[\mathbf{S} + j\omega_c \mathbf{R} - \omega_c^2 \mathbf{T}\right] \cdot \hat{\mathbf{E}}$$

with

$$\hat{f}_i = \mu_0 \int_\Omega \mathbf{W}_i \cdot \left[\frac{\partial \hat{\mathbf{J}}}{\partial t} + j\omega_c \hat{\mathbf{J}}\right] d\Omega \ . \qquad (23)$$

Matrices **R**, **S** and **T** are given by (4), ω_c denotes carrier angular frequency, and $\mathbf{W}_i$ is i-th vectorial weighting function. Finally $\mathbf{E}^\wedge = [\hat{e}_1, \hat{e}_2, ..., \hat{e}_N]^T$ is column vector of coefficients representing complex envelopes of electric field intensity, and $\mathbf{J}^\wedge = [\hat{j}_1, \hat{j}_2, ..., \hat{j}_N]^T$ is column vector of complex envelopes of source currents (13).

Applying Laplace transform to (22), we formally obtain the CFH equation (11), which is now formulated for images of complex envelopes $\mathbf{X}(s) = L\{\hat{\mathbf{e}}(t)\}$, and for $\mathbf{R}(s)$ we obtain

$$\mathbf{R}(s) = s\mathbf{T} \cdot \left[\hat{\mathbf{E}}_0 + \hat{\mathbf{E}}_0'\right] + \mathbf{B} \cdot \hat{\mathbf{E}}_0 + \hat{\mathbf{Q}}(s) \qquad (24)$$

with $\mathbf{Q}^\wedge(s) = L\{\mathbf{F}^\wedge(t)\}$.

Equation (11) for envelopes is then solved using CFH algorithm and Padé approximation.

The proposed method was used for modal analysis of the waveguide R100. One of side walls was removed (modeled by absorbing boundary condition), the others were perfectly electrically conductive. The finite-element mesh consisted of 44×20 rectangular cells.
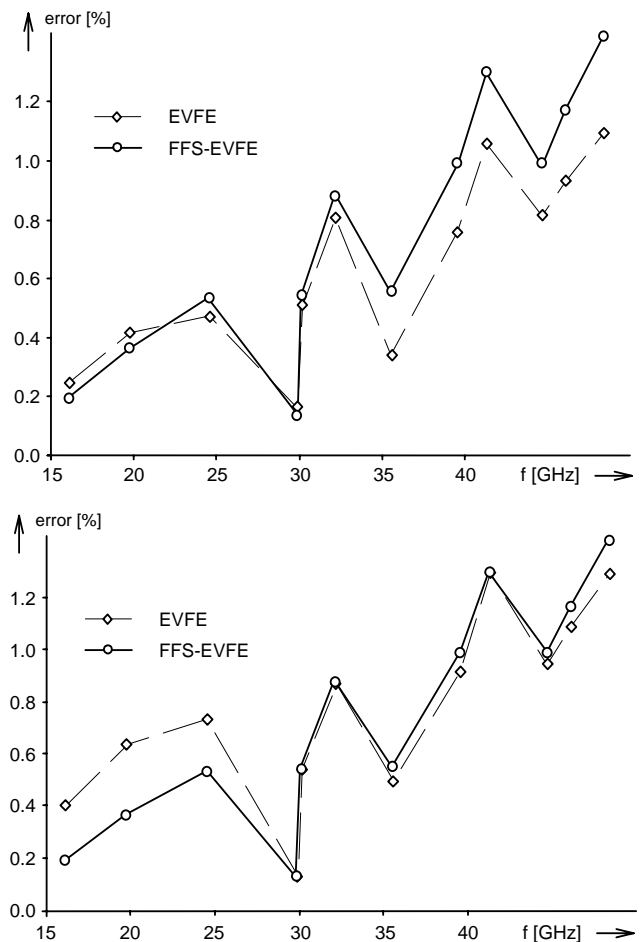
Fig. 7. Percentage error of the critical frequency of the waveguide R100 with removed side wall. Carrier frequency $f_c = 20$ GHz (top) and $f_c = 30$ GHz (bottom). Results of EVFE and FFS-EVFE are related to analytical computations.

Obviously, the percentage error is lower for FSS-EVFE in a short distance from the carrier frequency, and lower for EVFE in a longer distance from the carrier frequency.

Comparison of CPU-time demands of both the methods is rather complicated. EVFE demands depend on the frequency resolution of the analysis and are independent on the bandwidth of the analysis. On the contrary, FFS-EVFE demands are influenced by the width of the analyzed band and frequency resolution of the analysis does not play any important role [21], [30].

6. Conclusions

In the paper, original enhancements of time-domain finite elements for broadband modeling of microwave structures are proposed:

- Accuracy of the spatial approximation of the electromagnetic field distribution is improved by introducing original quasi-cubic basis and weighting functions. The smoothness of both the quasi-cubic approximation and its derivatives is another improvement.

- Accuracy of the temporal approximation of electromagnetic field has been assumed to be improved by introducing an original third-order polynomial approximation and resulting three-step algorithm for evaluating *new* time samples from existing ones. The proposed three-step algorithm does not exhibit better accuracy, but brings advantages in a more general formulation (the two-step algorithm is a special case of it).

- CPU-time demands of the finite-element analysis are reduced by the original exploitation of complex frequency hopping and Padé approximation. Thanks to the hops of complex frequency, the time of the analysis is approximately three-times shorter, and the accuracy is close to pure time-domain finite elements.

- Computation of parameters directly in the time domain is originally proposed in order to eliminate Fourier transforms of time-domain results. Time-domain broadband analysis is efficiently done using envelope finite elements, transversal field components are computed from longitudinal ones, and consequently, wave impedance is evaluated.

- Potential hybridization of different approaches is demonstrated by the original combination of envelope finite elements for the efficient broadband analysis and fast frequency sweep for further reduction of CPU-time demands.

All the described approaches were applied to the solution of the vectorial wave equation (1), which was converted to the matrix form by the finite-element procedure (3). The basic matrices stay unchanged for all the approaches, and (3) is slightly modified by basic matrix operations. This makes the algorithms simply implementable.

Acknowledgements

References

[1] ČERNOHORSKÝ, D., RAIDA, Z., ŠKVOR, Z., NOVÁČEK, Z. *Analýza a optimalizace mikrovlnných struktur (Analysis and Optimization of Microwave Structures)*. Brno: VUTIUM Publishing, 1999.

[2] VOLAKIS, J. L., CHATTERJEE, A., KEMPEL, L. C. *Fininte Element Method for Electromagnetics*. New York: IEEE Press, 1998.

[3] SILVESTER, P. P., FERRARI, R. L. *Finite Elements for Electrical Engineers*. Cambridge: Cambridge University Press, 1996.

[4] RAIDA, Z., TKADLEC, R., FRANEK, O., MOTL, M., LÁČÍK, J., LUKEŠ, Z., ŠKVOR, Z. *Analýza mikrovlnných struktur v časové oblasti (Time-Domain Analysis of Microwave Structures)*. Brno: VUTIUM Publishing, 2003.

[5] LEE, J.-F., LEE, R., CANGELLARIS, A. Time-domain finite element methods. *IEEE Transactions on Antennas and Propagation*. 1997, vol. 45, no. 3, p. 430–441.

[6] MOTL, M., FRANEK, O., RAIDA, Z. Comparison of time-domain finite element (TD-FE) and finite-difference time-domain (FDTD) methods. *In Proceedings of the International Symposium on Antennas JINA 2002*. Nice (France): S.E.E GRéCA, 2002, p. 79–82.

[7] TAFLOVE, A. *Computational Electrodynamics: The Finite-Difference Time-Domain Method* London: Artech House Publishing, 1995.

[8] TAFLOVE, A. *Advances in Computational Electrodynamics: The Finite-Difference Time-Domain Method*. Boston: Artech House Publishing, 1998.

[9] YEE, K. S. Numerical solution of initial boundary value problems involving Maxwell's equations in isotropic media. In *IEEE Transactions on Antennas and Propagation*. 1966, vol. 14, no. 3, p. 302 to 307.

[10] JIN, J *The Finite Element Method in Electromagnetics*. New York: John Wiley & Sons, 2002.

[11] LEE, J. F., SUN, D. K., CENDES, Z. J. Full-wave analysis of dielectric waveguides using tangential vector finite-elements. *IEEE Transactions on Microwave Theory and Techniques*. 1991, vol. 39, no. 8, p. 669–678.

[12] LEE, J. F. Finite element analysis of lossy dielectric waveguides. *IEEE Transactions on Microwave Theory and Techniques*. 1994, vol. 42, no. 6, p. 1025–1031.

[13] DUDLEY, D. G. *Mathematical Foundations for Electromagnetic Theory*. Piscataway: IEEE Press, 1994.

[14] CHEW, W. C., NASIR, M. A. A variational analysis of anisotropic, inhomogeneous dielectric waveguides. *IEEE Transactions on Microwave Theory and Techniques*. 1989, vol. 37, no. 4, p. 661–668.

[15] KOLBEHDARI, M. A., SRINIVASAN, M., NAKHLA, M. S., ZHANG, Q.-J., ACHAR, R. Simultaneous time and frequency do-

main solutions of EM problems using finite element and CFH techniques. *IEEE Transactions on Microwave Theory and Techniques*. 1996, vol. 44, no. 9, p. 1526–1533.

[16] RAIDA, Z. Finite-element complex-hopping analysis of microwave waveguides. In *Proceedings of the International Conference on Electromagnetics in Advanced Applications ICEAA '97*. Torino: Polytechnico di Torino (Italy), 1997, vol. 1, p. 163–166.

[17] WANG, Y., ITOH, T. Envelope finite element (EVFE) techniques – A more efficient time-domain scheme. *IEEE Transactions on Microwave Theory and Techniques*. 2001, vol. 49, no. 12, p. 2241–2247.

[18] TSAI, H. P., WANG, Y., ITOH, T. Efficient analysis of microwave passive structures using 3-D envelope finite element (EVFE). *IEEE Transactions on Microwave Theory and Techniques*. 2002, vol. 50, no. 12, p. 2721–2727.

[19] FRASSON, A. M. F., HERNANDEZ FIGUEROA, H. E. Envelope full-wave 3D finite element time domain method. *Microwave and Optical Components Letters*. 2002, vol. 35, no. 5, p. 351–354.

[20] JONES, D. C. *Methods in Electromagnetic Wave Propagation*. Oxford: Clarendon Press, 1979.

[21] MOTL, M. *Analysis of Microwave Structures by Variational Approaches*. Dissertation Thesis. Brno: Brno University of Technology, 2005.

[22] MOTL, M. High order approximation for finite element method in frequency and time domain. In *Proceedings of the 12th International Travelling Summer School on Microwaves & Lightwaves*. Minsk: Institute of Electronics of National Academy of Sciences of Belarus, 2002, p. 240–246.

[23] WEBB, J. P., FORGHANI, B. Edge elements and what they can do for you. *IEEE Transactions on Magnetics*. 1993, vol. 29, no. 2, p. 1460–1465.

[24] MOTL, M. Higher-order algorithm in time-domain finite element method. In *Proceedings of the 10th conference Student EEICT 2004*. Brno: Brno University of Technology, 2004, p. 114–118.

[25] POULARIKAS, A. D. *The Transforms and Applications Handbook*. Electrical Engineering Handbook Series. 2/E. Boca Raton: CRC Press, 2000.

[26] MOTL, M., FRANEK, O., RAIDA, Z. Comparison of finite element complex frequency hopping (FE/CFH) and finite-difference time-domain (FDTD) methods. In *Proceedings of the International Scientific Conference Radioelektronika 2002*. Bratislava: Slovak University of Technology, 2002, p. 70–73.

[27] MOTL, M., RAIDA, Z. Comparison of finite element complex frequency hopping (FEM/CFH) and time-domain finite element (TD-FEM) methods. In *Proceedings of the International Scientific Conference Radioelektronika 2003*. Brno: Brno University of Technology, 2003, p. 264–267.

[28] JORDAN, E. C., BAILMAN, K. G. *Electromagnetic Waves and Radiating Systems*, 2nd ed. Englewood Cliffs: Prentice Hall, 1968.

[29] MOTL, M., RAIDA, Z. Time-domain parameters of microwave transmission lines. In *Proceedings of the International Conference on Electromagnetics in Advanced Applications ICEAA 2003*. Torino: Politecnico di Torino, 2003, p. 147–150.

[30] MOTL, M., RAIDA, Z., LÁČÍK, J. Fast frequency sweep technique in envelope finite element method with absorbing boundary condition. *WSEAS Transactions on Computers*. 2004, vol. 3, no. 6, p. 1903 to 1906.

About Authors...

Milan MOTL was born in 1977 in Lanškroun. In 2001, he obtained master's degree in Electronics and Communication at Brno University of Technology. In 2005, he finished his dissertation thesis *Analysis of Microwave Structures by Variational Methods* to be defended at the same university. Since 2005, he is with the Flextronics Design occupying the position of RF design engineer. Mr. Motl is member of IEEE, and member of Radioengineering Society.

Zbyněk RAIDA – for biography, see p. 20 of this issue.

EUROPEAN MICROWAVE WEEK

Manchester – UK, September 10 – 15, 2006

Conference Topics:

- Microwave and Millimetre-wave Components: Technologies and Design
- Microwave Circuits and Sub-Systems
- Field Theory, Simulation Techniques and Methods
- Measurements, Electromagnetic Effects
- Antennas and Wave Propagation
- Microwave Systems and Applications

More Information:

- http://www.eumw2006.com

Deadlines:

- Submission of summaries: February 10, 2006
- Notification of acceptance: May 2, 2006
- Submission of full papers: June 9, 2006